Novel Dynamic Behavior of $Ce@C_{82}$ at Low Temperature

W. Sato, K. Sueki, K. Kikuchi, K. Kobayashi, S. Suzuki, Y. Achiba, and H. Nakahara
Graduate School of Science, Tokyo Metropolitan University, Hachioji, Tokyo 192-03, Japan

Y. Ohkubo
Research Reactor Institute, Kyoto University, Kumatori, Osaka 590-04, Japan

F. Ambe
The Institute of Physical and Chemical Research (RIKEN), Wako, Saitama 351-01, Japan

K. Asai
Department of Applied Physics and Chemistry, University of Electro-Communications, Chofu, Tokyo 182, Japan
(Received 14 July 1997)

Dynamic motion of $Ce@C_{82}$ in the forms of powder and *o*-dichlorobenzene solution is discussed based on time-differential perturbed angular correlation measurements. The observed angular correlations show the presence of two different chemical species of $Ce@C_{82}$. The temperature dependence of the reorientational correlation time abruptly changes at specific temperatures, implying the freezing of the molecular rotation. The data at low temperatures reveal that Ce stays at a certain site for one of the species, whereas for the other the atom has an intramolecular dynamic motion. [S0031-9007(97)04915-6]

PACS numbers: 61.48.+c, 36.40.Sx, 76.80.+y

Molecular dynamics of fullerenes has been investigated with various spectroscopic techniques [1–6] since the first macroscopic production of the species in 1990 [7], and it has generally been accepted that those inspected fullerene molecules have rapid and isotropic rotational motion at about room temperature even in solid form whether the carbon cages are encapsulating metal atom(s) or not.

In connection with molecular dynamics, the next concern is in the dynamic behavior of the encaged atom related to its intrinsic physical and chemical properties as in the carbon cage. Because the mobility of the encaged atom should highly depend on the strength of the chemical interaction between the ambient cage and the atom itself, we considered that the information pertaining to the dynamic motion of the encaged atom can be a significant clue to its chemical properties.

In order to elucidate the nature of fullerene dynamics and the chemical properties of an encapsulated atom as well as a carbon cage, a time-differential perturbed angular correlation (TDPAC) method was applied to $^{140}Ce@C_{82}$, a β^- decay product of $^{140}La@C_{82}$, which is produced by the neutron capture reaction of $^{139}La@C_{82}$. The TDPAC method was employed for the present paper as an exclusively useful spectroscopy among various analytical methods because it can provide direct information concerning the fluctuation of the principal axis of the electric field gradient (EFG) produced at the site of the probe nucleus, which possibly allows the evaluation of the magnitude of the EFG and/or the reorientational correlation time of the probe nucleus. Taking advantage of this method, we succeeded in observing the dynamic motion of the encaged Ce atom relative to the ambient cage.

Carbon soot containing La fullerenes was generated by a dc arc discharge of lanthanum-carbon composite rods in 250 torr He atmosphere. After solvent extraction of the fullerene ingredients from the soot, a two-step high-performance liquid chromatography (HPLC) separation was carried out with two different columns (a buckyprep column and a polystyrene column) in order to purify the fraction of interest. The fraction was identified as genuine $La@C_{82}$ by its UV-visible absorption spectrum [8]. About 3 mg of the purified sample was irradiated with reactor neutrons, with the neutron fluence rate of 1.0×10^{14} $cm^{-2}\,s^{-1}$ for 10 h, and radioactive $^{140}La@C_{82}$ was thereby produced. The samples in the forms of powder and *o*-dichlorobenzene solution (hereafter called "solid" and "solution" samples) were finally prepared by a HPLC purification with a buckyprep column to get rid of the impurities produced by hot atom effects and/or radiation effects [9].

The TDPAC measurements were performed at various temperatures (298, 240, 200, 160, 120, 100, 80, 40, and 10 K for the solid and 298, 280, 260, 240, 80, 40, and 10 K for the solution samples) on the 329–487 keV cascade γ rays from ^{140}Ce nucleus, whose 2083 keV intermediate state with its nuclear spin and parity of 4^+ has a half-life of 3.45 ns [10], by coincident detection of the two γ rays emitted toward 90° and 180° directions using BaF_2 scintillation counters. The TDPAC is expressed by the quantity $A_{22}G_{22}(t)$, where A_{22} $(= -0.14$ for the present case) is a coefficient characteristic of the relevant cascade transition and $G_{22}(t)$ is a time-differential perturbation factor. The $A_{22}G_{22}(t)$ was obtained from the number of coincident events, $N(\theta, t)$, observed at the angles, θ, of

90° and 180° by an equation, $A_{22}G_{22}(t) = 2\{N(\pi, t) - N(\pi/2, t)\}/\{N(\pi, t) + 2N(\pi/2, t)\}$ [11]. The details on the apparatus are described elsewhere [12,13].

$A_{22}G_{22}(t)$ spectra obtained for the solid and solution Ce@C_{82} at various temperatures are shown in Fig. 1. For the two Ce@C_{82} samples in different forms, the observed TDPAC spectra show the temperature dependence that reflects the effects of dynamic and static perturbation on the nuclear spin orientation by the extranuclear field [14–16]. At higher temperatures, respective spectra show exponential time-dependent attenuation of the angular correlation, which is typically observed when the reorientational correlation time of the EFG, τ_c, is sufficiently shorter than the reciprocal of the nuclear quadrupole frequency, $1/\omega_Q$. In this case, $G_{22}(t)$ is expressed by the following equation based on the diffusion approximation [17]:

$$G_{22}(t) = \exp(-\lambda t), \tag{1}$$

where

$$\lambda = 263 \tau_c \omega_Q^2 . \tag{2}$$

Here λ is the relaxation constant [18], which is proportional to $\tau_c \omega_Q^2$ in the case of electric quadrupole interaction, and t is the duration for which the nucleus is in the intermediate state of the cascade. At lower temperatures, on the other hand, the TDPAC spectra show oscillatory structures, implying the nuclear precession caused by a static perturbation. In the limiting static case for axial symmetry, $G_{22}(t)$ is defined by the conservation law of angular momentum as

$$G_{22}^{\text{static}}(t) = \frac{1}{3465}[993 + 30\cos(3\omega_Q t) + 243\cos(9\omega_Q t) + 540\cos(12\omega_Q t) + 525\cos(15\omega_Q t) + 588\cos(21\omega_Q t) + 378\cos(24\omega_Q t) + 168\cos(36\omega_Q t)]. \tag{3}$$

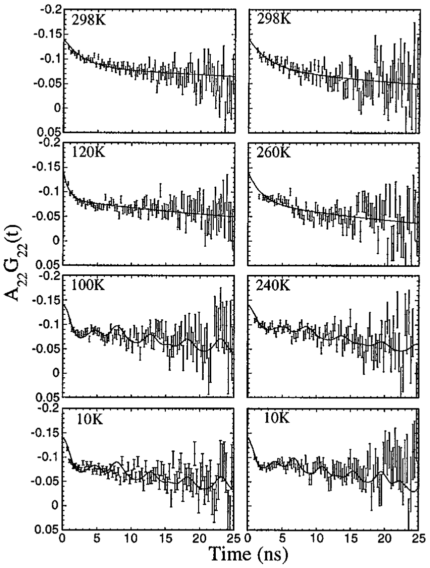

FIG. 1. Time variation of TDPAC of ^{140}Ce in Ce@C_{82}. The temperature-variant data on the left are for the solid Ce@C_{82} and those on the right are for Ce@C_{82} o-dichlorobenzene solution. Solid curves are best fitted with least squares using Eqs. (4) and (5) in the text.

Although the $A_{22}G_{22}(t)$ values for the higher temperatures are, according to Eq. (1), expected to become asymptotic to zero after a considerably long stay in the intermediate state, it appears that all of the spectra do not reach the asymptote. This observation evidently indicates that two different chemical species are present in the samples that give rise to a rapidly attenuating anisotropy and a slowly attenuating anisotropy. This interpretation could also be true of the data for the lower temperatures because the first dips of the anisotropy at about 3 ns do not reach zero in spite of the intrinsic properties of $G_{22}^{\text{static}}(t)$, and because the slow attenuation of the angular anisotropy observed at the higher temperatures can also be seen in the data. Moreover, we verified the presence of two different species by the fact that tentative simulated lines, assuming the presence of only one species, with an adiabatic approximation [16] do not reproduce the lower-temperature spectra. Therefore, taking these two different species into consideration and applying the above-stated two different $G_{22}(t)$ expressions by Eqs. (1) and (3), least squares fits were performed using the following equations [Eqs. (4) and (5)] for the $A_{22}G_{22}(t)$ data which show the typical exponential attenuation, at the higher temperatures, and those with the oscillatory structures, at the lower temperatures, respectively,

$$A_{22}G_{22}(t) = -0.14[P\exp(-\lambda_1 t) + (1 - P)\exp(-\lambda_2 t)] \tag{4}$$

and

$$A_{22}G_{22}(t) = -0.14[PG_{22}^{\text{static}}(t) + (1 - P)\exp(-\lambda_3 t)], \tag{5}$$

where the subscript numbers 1 and 2 stand for the first and second species, λ_3 is the relaxation constant of the second species observed at the lower temperatures, and P is the fraction of the first species. The fitted curves are shown in Fig. 1.

The ω_Q values optimized by the fits with Eq. (5) vary little in the low-temperature region and the average value $\langle\omega_Q\rangle$ for solid Ce@C_{82} [$= (6.5 \pm 0.3) \times 10^7$ rad s^{-1}] is in good agreement with that for the Ce@C_{82} o-dichlorobenzene solution [$= (7.2 \pm 0.7) \times 10^7$ rad s^{-1}] within their uncertainties. The same consequence was also obtained for the value of P: The average values, $\langle P\rangle$, for the solid and solution Ce@C$_{82}$ are 0.40 ± 0.03 and 0.42 ± 0.04, respectively. The values of each λ obtained for the solid and solution samples are plotted as a function of reciprocal temperature, $1/T$ in Fig. 2.

From the observation that the relaxation constants, λ_2 and λ_3, show smooth continuities from the higher to lower temperatures for both of the samples, the species which gives a slower relaxation constant, λ_2, at the higher temperatures is considered to correspond to the exponentially attenuating species at the lower temperatures. It is obvious for the higher temperatures that the values of λ_1 and λ_2 show almost the same temperature dependence, giving constant ratios of λ_1 to λ_2 at each observed temperature for both solid and solution samples of Ce@C$_{82}$, which could be proof that the two different chemical species have the same molecular rotational mode. By analogy with the rotational motion of C$_{60}$, it is reasonable to assume that not only Ce@C$_{82}$ in o-dichlorobenzene solution but solid Ce@C$_{82}$ is also rotating randomly at the higher temperatures, and that the abrupt change of the temperature dependence between λ_2 and λ_3 at about 80 K is attributed to the freeze of the molecular rotation. This presumption is strongly supported by the observation that the temperature dependence of these λ for the solution Ce@C$_{82}$ changes at about the melting point of o-dichlorobenzene, 256 K. The activation energies in the range of the presumed molecular rotation were estimated by least squares fits on an Arrhenius type equation as 1.3 ± 0.1 and 5.9 ± 1.4 kJ mol^{-1} for the solid and solution samples, respectively. The difference in the values might indicate that Ce@C$_{82}$ solvated by o-dichlorobenzene molecules needs more energy for its thermal rotation.

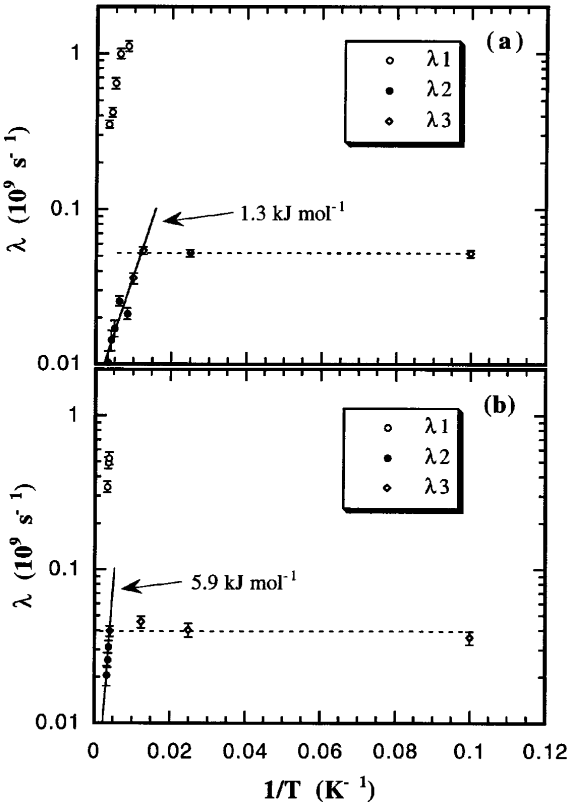

FIG. 2. Temperature dependence of the relaxation constants (λ_1, λ_2, and λ_3) for (a) solid Ce@C$_{82}$ and (b) solution Ce@C$_{82}$. The dotted horizontal lines indicate the average values of each λ_3.

At the temperatures lower than the freezing point of the rotational motion, the observed $A_{22}G_{22}(t)$ data clearly indicate that both statically and dynamically perturbed species coexist in each of the samples. Taking into consideration the freezing of the molecular rotation, it can be inferred that for the first chemical species the encaged Ce atom has a tight bonding with the ambient carbon cage while staying at the intermediate state of the cascade, and therefore they are statically perturbed to make a nuclear precession. On the other hand, the second species, with its angular correlation exponentially attenuating, undoubtedly has a dynamic motion even after the freezing of the molecular rotation. Below the freezing point, however, the cause of the dynamic perturbation on the Ce nucleus can not be ascribed to the motion of the whole molecule, such as its hopping among the lattice sites, because despite different interactions with the surrounding molecules, the observed data give the same λ_3 values for the solid and solution samples within their uncertainties. In addition, it is difficult to regard the movement as thermally activated motion because little, if any, temperature dependence was observed in the low-temperature range for both samples. From this inductive inference, intramolecular dynamic motion of the encapsulated Ce atom lasting at least for the time scale of a nanosecond is nominated for certain as the cause of the attenuation of the angular correlation. Taking into account the little, if any, temperature dependence at the lower temperatures, this novel dynamic behavior of the encaged atom is considered to be caused by the recoil effect triggered by the β^- decay from ^{140}La and, to a lesser degree, by the emission of the first γ ray, namely, the Ce atom jumps out of the potential produced by the interaction between the atom itself and the ambient carbon cage. (It should be noted that carbon cages are already reported to be very stable against the impact of the collision of atoms with its recoil energy of β^- decay [19].) In this case, it is most plausible to consider that the Ce ion is making a loop motion along the wall of the cage [20,21] because irregular movement by elastic and/or inelastic collisions against the wall of the carbon cage would completely dissipate the initial recoil energy within the femtosecond or picosecond time scale [22]. In this way, the atom is considered to roll along the wall of the cage for enough time to allow the TDPAC to be measured even though there are electrostatic energy barriers along the path of the atom.

Assuming a model with the $\langle P \rangle$ values for each of the samples representing the fractions of the Ce@C$_{82}$ with the encapsulated Ce atom attached to a certain position of the ambient carbon cage, and the other Ce@C$_{82}$ with the

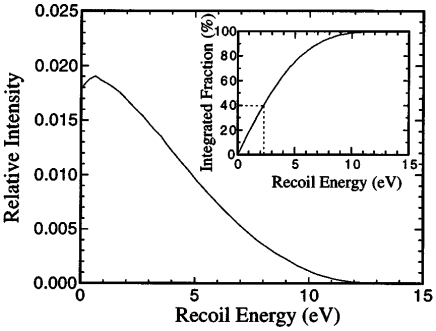

FIG. 3. Energy distribution of the encaged Ce atoms induced by the recoil effect of the β^- particle emission from ^{140}La. The inset shows the integrated fraction of the number of atoms as a function of the recoil energy.

Ce atom having received the recoil energy higher than a threshold value is the second species, the threshold energy for the latter can be estimated to be 2.3 eV from the recoil energy distribution caused by the β^- particle emission shown in Fig. 3. This value is in good agreement with a calculated value, about 54 kcal mol^{-1}, for La@C$_{82}$ [23].

In the present paper, the following were empirically and analytically ascertained: (1) There are two different chemical species produced after the β^- decay and their behaviors on the $A_{22}G_{22}(t)$ data are remarkably different from each other. (2) At the higher temperatures, Ce@C$_{82}$ molecules are rotating even in the solid form and the correlation time showed a temperature dependence as has already been reported. (3) The $A_{22}G_{22}(t)$ data at the lower temperatures obviously show a certain effect of dynamic perturbation of the system as well as that of static. These observations suggest that the intramolecular dynamic motion of the encapsulated atom inside the fullerene cage is initiated by the recoil energy of the β^- particle emission and lasts for the time scale of these TDPAC measurements.

We appreciate helpful discussions with Professor S. Nagase. We are also grateful to Professor M. Katada for his deep interest in this paper. This paper was partly supported by a grant from the Ministry of Education, Culture, Sports, and Science of Japan.

[1] C. S. Yannoni *et al.,* J. Phys. Chem. **95**, 9 (1991).
[2] R. Tycko *et al.,* J. Phys. Chem. **95**, 518 (1991).
[3] R. Tycko *et al.,* Phys. Rev. Lett. **67**, 1886 (1991).
[4] Y. Maniwa *et al.,* Solid State Commun. **80**, 609 (1991).
[5] R. D. Johnson *et al.,* Science **255**, 1235 (1992).
[6] N. Okabe *et al.,* Appl. Magn. Reson. **10**, 251 (1996).
[7] W. Krätschmer *et al.,* Nature (London) **347**, 354 (1990).
[8] K. Kikuchi *et al.,* Chem. Phys. Lett. **216**, 67 (1993).
[9] K. Sueki *et al.,* J. Radioanal. Nucl. Chem. (to be published).
[10] *Table of Isotopes,* edited by R. B. Firestone and V. S. Shirley (Wiley, New York, 1996), Vol. 1, 8th ed.
[11] E. Gerdau *et al.,* Z. Phys. **263**, 5 (1973).
[12] Y. Ohkubo *et al.,* Phys. Rev. B **47**, 11 954 (1993).
[13] Y. Ohkubo *et al.,* J. Phys. Chem. **99**, 10 629 (1995).
[14] M. Blume, Nucl. Phys. **A167**, 81 (1971).
[15] R. M. Lyndenn-Bell, Mol. Phys. **21**, 891 (1971).
[16] A. G. Marshall and C. F. Meares, J. Chem. Phys. **56**, 1226 (1972).
[17] A. Abragam and R. V. Pound, Phys. Rev. **92**, 943 (1953).
[18] The numerical value, 263, was obtained from Eq. (71) in Ref. [17] by substituting 4 for I and 2 for k.
[19] K. Kikuchi *et al.,* J. Am. Chem. Soc. **116**, 9775 (1994).
[20] K. Kobayashi, S. Nagase, and T. Akasaka, Chem. Phys. Lett. **261**, 502 (1996).
[21] W. Andreoni and A. Curioni, in *Theory of (La, Y) Endohedrally Doped Fullerenes: The Past and the Present,* edited by W. Andreoni, The Chemical Physics of Fullerenes 10 (and 5) Years Later (Kluwer, The Netherlands, 1996).
[22] G. Harbottle, in *Effects of Nucleogenesis Preceding Chemical Reaction: Dissipation of Excitation Before Chemical Reaction*, edited by G. Harbottle and A. G. Maddock, Chemical Effects of Nuclear Transformations in Inorganic Systems (North-Holland, Amsterdam, 1979).
[23] S. Nagase *et al.,* Chem. Phys. Lett. **201**, 475 (1993).